MSDE

PAPER

View Article Online
View Journal | View Issue

Cite this: *Mol. Syst. Des. Eng.*, 2025, **10**, 40

Enhanced glucose-responsivity of PBA–diol hydrogel networks by reducing crosslink affinity†

Sijie Xian, Yuanhui Xiang, Svenja Deichmann and Matthew J. Webber *

Received 30th June 2024,
Accepted 10th October 2024

DOI: 10.1039/d4me00106k

rsc.li/molecular-engineering

Glucose-responsive hydrogel systems are increasingly explored for insulin delivery, with dynamic-covalent crosslinking interactions between phenylboronic acids (PBA) and diols forming a key glucose-sensing mechanism. However, commonly used PBA and diol chemistries often have limited responsiveness to glucose under physiological concentrations. This is due, in part, to the binding of PBA to the commonly used diol chemistries having higher affinity than for PBA to glucose. The present study addresses this challenge by redesigning the diol chemistry in an effort to reduce its binding affinity to PBA, thereby enhancing the ability of glucose to compete with these redesigned PBA–diol crosslinks at its physiological concentration, thus improving responsiveness of the hydrogel network. Rheological analyses support enhanced sensitivity of these PBA–diol networks to glucose, while insulin release likewise improves from networks with reduced crosslink affinities. This work thus offers a new molecular design approach to improve glucose-responsive hydrogels for insulin delivery in diabetes management.

Design, System, Application

Dynamic-covalent bonds are a class of equilibrium-governed interactions that have been explored for the preparation of hydrogel networks with emergent dynamic properties. One specific class, the bond formed between phenylboronic acids and diols, has been used for several decades to prepare glucose-responsive materials. However, the resulting bonds are not often sensitive to glucose under physiological concentrations, as the affinity between PBA and the diol used to form the network far exceeds that for the PBA binding to glucose. The present study explores a variety of different diol crosslinking chemistries, with the goal of restoring network responsivity. Certain diols produce hydrogel networks with more glucose-dependent mechanical properties, translating to glucose-directed release of encapsulated insulin. Of specific design relevance, the best-performing networks arise from diol structures with reduced affinity for PBA. Accordingly, this work points to a new design rationale for the preparation of glucose-responsive materials that uses reduced network crosslink affinity to prepare materials for more autonomous delivery of insulin in response to changes in glucose levels, toward better management of diabetes.

1. Introduction

Hydrogels are three-dimensional polymer networks that can imbibe significant amounts of water while maintaining their physical structure, making them ideal for drug delivery and biomedical applications.[1–3] These materials are often categorised by their mode of crosslinking, and commonly use either chemical crosslinking, which involves covalent bond formation, or physical crosslinking, which arises from dynamic/reversible interactions or entanglements.[4,5] Hydrogels crosslinked by dynamic and equilibrium-governed interactions, such as supramolecular motifs or non-covalent associations,[6,7] typically exhibit emergent dynamics on the bulk scale leading to properties such as shear-thinning and self-healing for injection-centered application.[8] However, the use of such dynamic interactions often comes with mechanical properties that are weaker than covalently crosslinked analogues. Dynamic-covalent bonds, a class of equilibrium-governed covalent interactions,[9] offer an opportunity to capture features of both chemical and physical crosslinking in constructing hydrogels with improved mechanical properties that, at the same time, benefit from dynamic bond exchange leading to shear-thinning and self-healing character.[10]

Boronate esters formed between phenylboronic acids (PBAs), a class of Lewis acids, and *cis*-1,2 or *cis*-1,3 diols have been broadly explored for their ability to form dynamic-covalent hydrogel networks, with the equilibrium bond formation of these interactions dictated by temperature, pH, or the presence of competing diol species.[11–18] In the context of insulin delivery,

Department of Chemical & Biomolecular Engineering, University of Notre Dame, Notre Dame, IN 46556, USA. E-mail: mwebber@nd.edu

† Electronic supplementary information (ESI) available: Detailed synthetic methods, schemes, and ^{1}H NMR characterization data; acid–base titration; isothermal titration calorimetry (ITC); ESI-MS; rheology; release study. See DOI: https://doi.org/10.1039/d4me00106k

this crosslinking chemistry has long been evaluated in the preparation of hydrogel networks that are subject to competition from free glucose, a *cis*-1,2 diol, to yield a reduction in crosslink density as glucose levels increase.[19–24] Of specific importance in designing PBA-based glucose recognition is the pK_a of the boronic acid, defining the pH for transition from the neutral trigonal to charged tetrahedral boronate species; without electron-withdrawing substituents, PBAs have a pK_a of ~8.8.[13] Under aqueous conditions, the boronate ester formed between diols and a tetrahedral boronate is the most stable species, enabling the equilibrium to be shifted to the PBA–diol bound form.[18] Numerous efforts have been made to explore inclusion of electron-withdrawing substituents, intermolecular interactions, or adjacent charged groups to reduce pK_a and enable efficient PBA–diol recognition under normal physiological conditions.[25–28] Commonly, PBAs with fluorine substitutions have been used, enabling a reduction in pK_a to ~7.2 for stable boronate ester bonds under physiological conditions.[29,30] In spite of some potential for use in glucose-responsive insulin delivery, PBAs have a number of remaining drawback. These include a lack of specificity for glucose, meaning PBAs will bind to a variety of other physiologically relevant diol species.[18] In addition, PBAs have a high affinity for commonly used diol crosslinkers, such as the glucose-like diol (GLD) derived from reaction of amino groups with glucano-δ-lactone,[11] that limit competition-mediated bond rupture by free glucose. A recent study showed the binding affinity for this commonly used PBA–diol crosslinking motif was 4.9×10^3 M^{-1}, whereas the affinity of the same PBA motif for glucose was only 8.6 M^{-1}.[31] Efforts to improve both the affinity and specificity of the PBA–glucose interaction have been an active area of discovery, including recent reports of diboronate motifs that offer high-affinity, bidentate recognition of glucose without increased affinity for common competing analytes.[31,32] The use of this diboronate facilitated glucose recognition with physiologically relevant affinity, enhancing the function and glucose-responsiveness of materials and formulations formed from diboronate–diol bonds.

The current study takes a different approach to enhancing the glucose-responsive sensitivity of PBA–diol crosslinks, exploring multiple *cis*-1,2 and *cis*-1,3 diol derivatives designed to reduce crosslinking affinity to a model PBA molecule (Fig. 1). The binding of PBAs to diol derivatives follows the typical trend in binding affinity: *cis*-1,2 diols > *cis*-1,3 diols ≫ *trans*-1,2 diols. In this study, various *cis*-1,2 and *cis*-1,3 diol derivatives were designed and investigated, including diols derived from glucose and fructose, which are known to bind effectively to PBAs, as well as synthetic diols prepared *via* epoxide ring-opening reactions. Analysis at both the molecular and material scales reveal certain diol derivatives to have lower binding affinities to a model PBA than are typical for the traditionally used GLD chemistry. By reducing crosslinking affinity, glucose is better able to compete with these interactions, enhancing sensitivity of the resulting PBA–diol dynamic-covalent networks. Accordingly, whereas previous

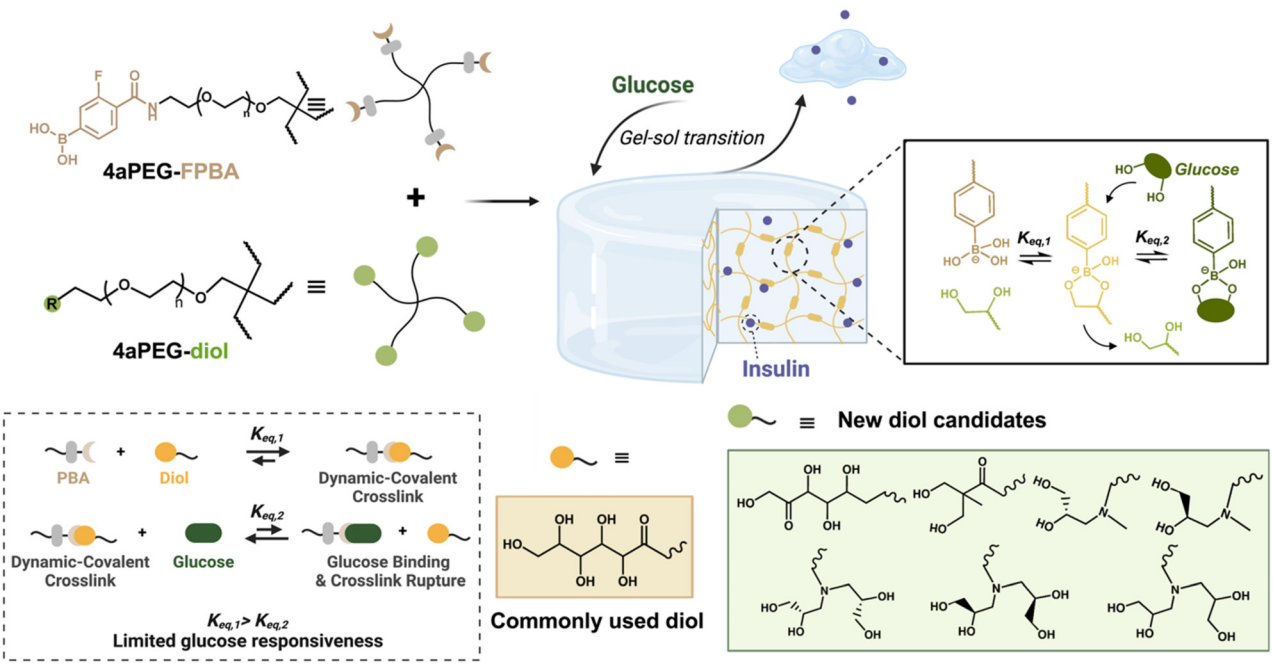

Fig. 1 Schematic illustration of PBA–diol dynamic-covalent hydrogel networks prepared from 4-arm PEG (4aPEG) terminated with PBA or diol groups and encapsulating insulin cargo. As glucose levels increase, free glucose competitively displaces the dynamic-covalent PBA–diol crosslinks, leading to insulin release due to disruption of the hydrogel network. The binding affinity of PBA to a commonly used glucose-like diol is significantly higher than to glucose, limiting the glucose-responsive function of the resulting hydrogels. Several new diol chemistries were designed here to explore the responsivity of networks prepared from alternative PBA–diol crosslinking.

works have sought to improve responsivity of this class of networks by increasing the glucose-binding affinity of the PBA motif, the present study instead demonstrates improved network responsivity by lowering the affinity of crosslinks comprising the network junctions. Accordingly, this approach suggests a new design rationale to better engineer glucose-responsive materials for insulin delivery.

2. Experimental methods

2.1. Synthesis of model compounds and macromers

Details for the synthesis of all molecules and 4-arm polyethylene glycol (4aPEG) macromers, as well as molecular characterization data (Fig. S1–S13†), can be found in the online supporting information. Fluorine-modified 4-carboxy-3-fluorophenylboronic acid (FPBA) was selected as the model boronate derivative for exploration here, and studied for its binding to the commonly used glucose-like diol (GLD) chemistry as well as a variety of different modified diol chemistries, including a fructose-like diol (FLD) appended to the 4aPEG *via* click chemistry as well as a series of diols prepared from epoxide ring-opening reactions of glycidol compounds with 4aPEG macromers bearing terminal primary or secondary amines.

2.2. Glucose dependent rheological characterization

Hydrogels were prepared from 4aPEG-FPBA and each diol-modified 4aPEG macromer at 1 : 1 by mole in terms of the end-groups on each macromer and under varying glucose concentrations (0 mg dL^{-1}, 100 mg dL^{-1}, 200 mg dL^{-1}, and 400 mg dL^{-1}) in 30 mM phosphate buffer (pH 7.45, 22.6 mM disodium phosphate and 7.4 mM monosodium phosphate with 120 mM NaCl) at the desired total polymer concentration, typically 10% (w/v). As pH directly dictates the extent of bonding in PBA–diol networks,[11] this buffer ensured constant pH for all experiments. The mechanical properties of the hydrogels were assessed using a TA Instruments HR-2 rheometer equipped with a Peltier stage set to 25 °C. Measurements were conducted with a 25 mm parallel plate geometry using a gap height of 200 μm. Initial oscillatory strain amplitude sweep measurements were collected from 0.1% to 100% strain with 10 points per decade at a frequency of 30 rad s^{-1} to verify the linear viscoelastic region for all materials. Subsequently, oscillatory frequency sweep measurements were collected from 0.1 rad s^{-1} to 200 rad s^{-1} with 10 points per decade at 1% strain. All measurements were at 25 °C.

2.3. Glucose dependent FITC-insulin release study

To evaluate glucose-dependent insulin release from hydrogel networks, 100 μL hydrogels were prepared from FPBA- and diol-modified 4aPEG macromers at 1 : 1 by mole in terms of the end-groups on each macromer in phosphate buffer at 10% (w/v) total polymer concentration. To each hydrogel, 200 μg of a FITC-labelled insulin was added, synthesized as previously described.[14] Briefly, FITC-labelled insulin was first dissolved and thoroughly mixed in the FPBA-modified 4aPEG macromer solution. Diol-modified 4aPEG macromers were then added to this mixture to form hydrogels as described above. Gels were prepared in circular molds placed within 12-well plates and immersed in 4 mL of pH 7.4 release buffer containing 0, 100, or 400 mg dL^{-1} glucose. At each time point, a 20 μL aliquot of the bulk phase was taken and further diluted to 200 μL for fluorescence analysis (ex: 485 nm, em: 520 nm) on a Tecan M200 plate reader. At each sampling, the bulk was adjusted by replacement with 20 μL of the same release buffer to maintain constant volume. FITC-insulin concentrations at each time were determined using a standard curve, and data was processed to reflect cumulative release. After 8 h, gels were manually destroyed by treating with HCl solution to disrupt any remaining gel network and free residual FITC-insulin. The pH of this mixture was adjusted to pH 7.4 and insulin was quantified for mass balance closure.

2.4. Isothermal titration calorimetry

The binding affinities (K_{eq}) between FPBA and each diol derivative in their small molecule form were measured by isothermal titration calorimetry (ITC). All titration experiments were performed at 298 K on a PEAQ-ITC calorimeter (Microcal, Inc.) in degassed pH 7.4 PBS buffer, using a 38 μL syringe and 200 μL cell and consisting of 19 injections. The measurements were performed by titrating diol derivatives from the syringe into a solution of FPBA loaded in the cell at concentrations suitable for the affinity of each interaction, as further summarized in Table S1.† The first injection, 0.4 μL of diol derivative was added to FPBA in the cell over a duration of 0.8 s; this injection was removed from analysis. For each subsequent injection, 2 μL of each diol derivative was delivered to the cell over a duration of 4 s, with a 150 s interval between injections. All raw data were corrected by subtraction of a dilution measurement of the titrated diols into buffer and were then subjected to global analysis, fitting, and graphing using the integrated public-domain software packages of NITPIC, SEDPHAT, and GUSSI.[33] NITPIC performs unbiased integration, baseline correction, and error estimates for accurate data weighting during fitting. SEDPHAT is then used for data analysis and model fitting. GUSSI generates graphs of these processed ITC results. The "A + B ⟷ AB hetero-association" model was used in the SEDPHAT data fitting process, with "B" representing the diol derivative in the syringe in all cases. It is important to note that the PBA–diol interaction is relatively weak. The estimated Wiseman '*c*' parameter for many of the systems characterized here is approximately 1.5, and thus below the optimal "experimental window." This results in unsaturated and non-sigmoidal titration curves. While the binding affinity for such low-affinity interactions can still be accurately derived, enthalpy values should be interpreted with with caution due to the limitations of the titration curve shape and low *c*-values.[34,35]

3. Result and discussion

3.1. Material synthesis and characterization

To better study dynamic-covalent interactions between PBA and diol derivatives, 4aPEG macromers containing either FPBA groups (4aPEG-FPBA; 85% modification) or diol derivatives were synthesised by modifying the end groups of 10 kDa 4aPEG macromers at high modification percentages, as quantified by ^{1}H NMR. The use of 4aPEG macromers enables formation of ideal-like network structures to simplify study of network crosslinking.[12] In total, eight different diol derivatives were assessed, including those bearing the traditional GLD (4aPEG-GLD; 80% modification), a fructose-like diol (4aPEG-FLD; 80% modification), a *cis*-1,3 diol (4aPEG-D-1,3; 70% modification), different *cis*-1,2 diols prepared from either an S-type (4aPEG-D-1,2(*S*); 73% modification) or R-type (4aPEG-D-1,2(*R*); 76% modification) stereoisomeric glycidol, or a double *cis*-1,2 diol structure prepared from S-type (4aPEG-Du-1,2(*S*), 95% modification), R-type (4aPEG-Du-1,2(*R*), 91% modification), or racemic (4aPEG-Du-1,2(*SR*), 95% modification) glycidol precursors. The structures of each of these diols are depicted in Fig. 1, with detailed methods for their synthesis, route of attachment to 4aPEG macromers, and corresponding ^{1}H NMR characterization available in the online supporting information. The efficiency of the various 4aPEG modification reactions stems from the different conjugation routes employed. Macromers synthesized *via* two epoxide ring-opening reactions on the primary amine-bearing 4aPEG-NH_2—namely, 4aPEG-Du-1,2(*S*), 4aPEG-Du-1,2(*R*), and 4aPEG-Du-1,2(*SR*)—proved to be highly efficient. In contrast, the synthesis of other macromers, which required two-step preparation protocols (4aPEG-D-1,2(*S*), 4aPEG-D-1,2(*R*), and 4aPEG-FLD), carbodiimide couplings (4aPEG-FPBA and 4aPEG-D-1,3), or ring-opening aminolysis (4aPEG-GLD), exhibited lower efficiency, likely arising from less efficient reaction schemes. Nonetheless, in all cases, all macromers were functionalized above the threshold necessary for network formation.[36]

3.2. Verification of gelation

An initial gelation test was performed by mixing 4aPEG-FPBA with each diol macromer at a molar ratio of 1 : 1 on the basis of the end groups of each macromer. Prior work reported networks from the FPBA–GLD interaction at 10% (w/v) total polymer in water,[11] yet these hydrogels had very limited glucose responsive function. This concentration was thus deemed a good benchmark to explore the ability of alternate diol chemistries to rescue glucose-responsiveness in these networks. Moreover, calculations performed for 4aPEG macromers suggest 10% (w/v) to be just below the overlap concentration (c*), thereby enabling study of the impact of dynamic-covalent crosslinks with limited consideration for chain entanglements.[31] As such, samples were prepared by mixing each of the eight different diol-modified 4aPEG macromers with the 4aPEG-FPBA macromer at a total polymer concentration of 10% (w/v) in phosphate buffer at pH 7.4, in order to first assess hydrogelation and establish a basis to determine whether responsiveness could be "rescued" by using new diol chemistries. The samples were first qualitatively assessed for their ability to form self-supporting hydrogel networks (Fig. 2). According to gross assessment by vial inversion, five out of the eight diol derivatives formed hydrogels within 30 s of mixing the macromers. As expected, the previously reported 4aPEG-GLD macromer formed a stable self-supporting hydrogel. Similarly, 4aPEG-FLD, prepared from the fructose-like diol, also formed a hydrogel network upon mixing with 4aPEG-FPBA. The 4aPEG-D-1,3 material did not form a self-supporting hydrogel network; this aligns with the expected trends in binding affinity of PBAs of *cis*-1,2 diols > *cis*-1,3 diols ≫ *trans*-1,2 diols.[37] Indeed, this binding preference demonstrates that the arrangement of the hydroxyl groups is crucial for effective PBA binding. A single *cis*-1,2 diol derivative was next tested for hydrogelation, having either *S*-stereochemistry, 4aPEG-D-1,2(*S*), or *R*-stereochemistry, 4aPEG-D-1,2(*R*). This modification was prepared by an epoxide ring-opening reaction between a stereoisomeric glycidol molecule and a 4aPEG bearing terminal secondary amines.

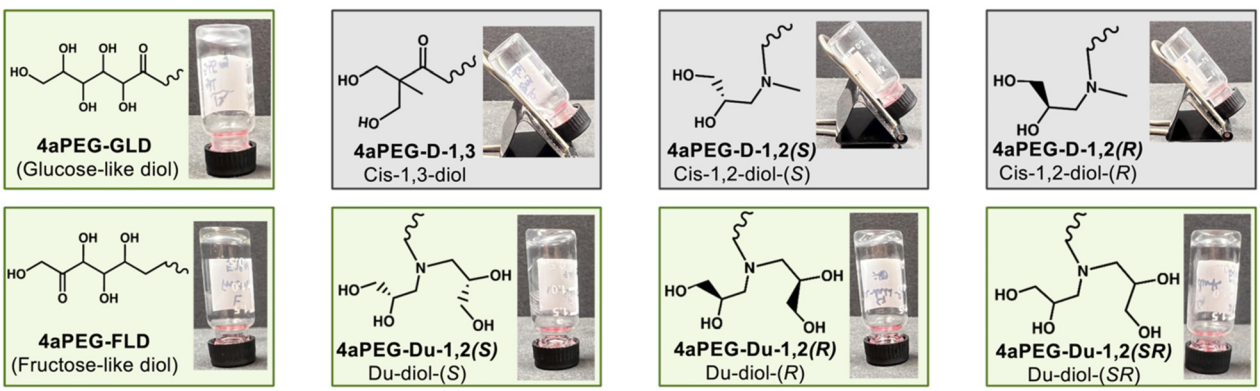

Fig. 2 Hydrogel screening *via* vial inversion of 10% (w/v) mixtures in phosphate buffer (0.1 M, pH 7.4) of 4aPEG-FPBA and different 4aPEG-diols, consisting of 4aPEG-GLD, 4aPEG-FLD, 4aPEG-D-1,3, 4aPEG-D-1,2(*S*), 4aPEG-D-1,2(*R*), 4aPEG-Du-1,2(*S*), 4aPEG-Du-1,2(*R*), or 4aPEG-Du-1,2(*SR*). Green boxes indicate samples that formed self-supporting hydrogels.

However, neither of these single *cis*-1,2 diol structures formed self-supporting hydrogels when mixed with 4aPEG-FPBA. This may be explained by the mechanism of epoxide ring-opening of glycidol molecules used to modify the macromer; though expected to open primarily from the less substituted side *via* an S_N2 reaction to yield the *cis*-1,2 diol,[38–43] some fraction may instead open from the more substituted side to yield a *cis*-1,3 diol (Fig. S14†). As an average of at least 3 arms must be crosslinked for a 4aPEG macromer to form a continuous network, any sites modified with a *cis*-1,3 diol instead would likely compromise gelation given the modification percentages of these macromers and the reduced affinity of the *cis*-1,3 species. To ensure a greater propensity for crosslinking in spite of the possible occurrence of some fraction of *cis*-1,3 diols upon ring-opening, a second approach was taken using a ring-opening reaction between the same glycidol molecules and a 4aPEG bearing terminal primary amines to enable two ring-opening reactions at each macromer terminal group. From this approach, three double-modified *cis*-1,2-diol enantiomers (*S*-, *R*-, and racemic mixture) were prepared, resulting in macromers of 4aPEG-Du-1,2(*S*), 4aPEG-Du-1,2(*R*), and 4aPEG-Du-1,2(*SR*) that all formed self-supporting hydrogel networks with 4aPEG-FPBA. No significant differences were observed among the enantiomers in terms of their ability to form stable hydrogels upon gross inspection.

3.3. Glucose-responsive hydrogel properties

The diol derivatives that formed self-supporting hydrogels upon mixing with 4aPEG-FPBA were further evaluated to assess their glucose-responsive dynamic properties using oscillatory rheology. Hydrogels were formulated as before, at 10% (w/v) in pH 7.4 buffer with a 1 : 1 molar ratio on the basis of the functionalized arms of each macromer. The glucose concentration of the buffer was selected to be 0, 100, 200, and 400 mg dL^{-1}, capturing physiological levels ranging from normoglycemic to hyperglycemic conditions. As glucose level is increased, a glucose-responsive hydrogel would be expected to exhibit a reduction in its modulus as glucose competes with PBA–diol crosslinks comprising the network junctions; glucose competition also should result in increased hydrogel dynamics.[31] As such, hydrogels were assessed for frequency-dependent properties of their storage (G') and loss (G'') moduli, and furthermore compared on the basis of their apparent high-frequency plateau modulus (G_0), compared at 20 rad s^{-1}, under each glucose condition (Fig. 3). For dynamic hydrogels, the modulus in the high-frequency regime is a function of the equilibrium extent of network crosslinking.[4]

The hydrogels prepared from 4aPEG-GLD formed the expected stiff network in the absence of glucose, with a value

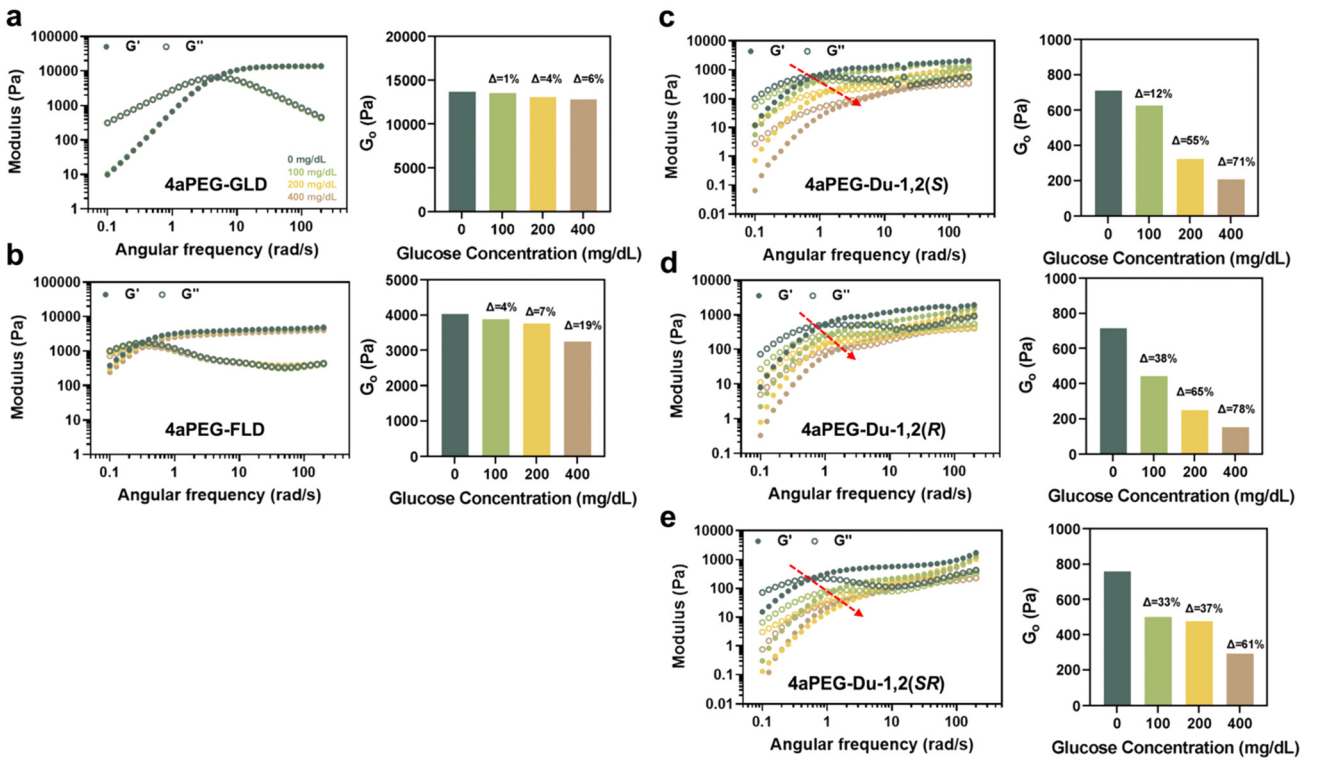

Fig. 3 Glucose-dependent oscillatory rheology frequency sweeps (left) and comparative G' values (at 20 rad s^{-1}) for hydrogels prepared from 4aPEG-FPBA and different 4aPEG-diols, consisting of (a) 4aPEG-GLD, (b) 4aPEG-FLD, (c) 4aPEG-Du-1,2(*S*), (d) 4aPEG-Du-1,2(*R*), or (e) 4aPEG-Du-1,2(*SR*). All samples were prepared at 10% (w/v) in phosphate buffer (0.1 M, pH 7.4). Glucose values ranged from 0–400 mg dL^{-1}. For frequency sweeps, G' (closed circles) and G'' (open circles) are both plotted. Red arrows indicate trends for the shift in the G'–G'' crossover (ω_c) in more responsive hydrogels.

for G' of 1.4×10^4 Pa (Fig. 3a). This measurement is of the same order as that previously reported for this same chemistry.[11] As was also previously described for this material at 10% (w/v),[31] it had limited glucose-responsive character as G' decreased by only 6% when prepared in a high glucose condition of 400 mg dL^{-1}. Similarly, there was no observed change in network dynamics on the basis of the G'–G'' crossover point (ω_c) for the glucose conditions evaluated; ω_c was approximately 5 rad s^{-1} for samples prepared across the different glucose levels. The timescale for network relaxation ($\tau_r = 2\pi/\omega_c$) evident from this crossover was thus approximately 1.3 s. Comparatively, the network prepared from 4aPEG-FLD had a stiffness that was about an order of magnitude lower (4×10^3 Pa), and G_0 demonstrated a 19% reduction when increased to a glucose level of 400 mg dL^{-1} (Fig. 3b). In terms of network dynamics, the apparent τ_r for the network prepared by FLD in the absence of glucose was 19.9 s. Interestingly, the network formed from the FLD structure was thus about one order of magnitude less dynamic than the network formed from GLD. Accordingly, the network stiffness and the rates of underlying bond exchange are decoupled, and constitute separate diol-dependent features of PBA–diol networks. For crosslinked ideal-like networks, k_{off} can be estimated from $1/\tau_r$;[44,45] thus, the FLD networks had a k_{off} of 0.05 s^{-1} while the GLD network had more rapid bond exchange with a k_{off} of 0.80 s^{-1}.

The networks prepared by combining the 4aPEG-FPBA macromer with macromers of 4aPEG-Du-1,2(*S*), 4aPEG-Du-1,2(*R*), and 4aPEG-Du-1,2(*SR*) that had two *cis*-1,2 diols on each arm exhibited a significantly reduced modulus in the absence of glucose, in all cases in the range of 7×10^2 Pa (Fig. 3c–e). The plateau storage modulus decreased by 71% (*S*), 78% (*R*), and 61% (*SR*) at 400 mg dL^{-1} glucose. The crosslinks in these hydrogels were thus much more susceptible to competition from glucose than were those in either of the networks prepared from GLD or FLD crosslinking chemistries. In the absence of glucose, the values of ω_c in these three networks were all similar, in the range of 1 rad s^{-1}, corresponding to a value of τ_r of 6.3–7.9 s, and indicating a k_{off} for network crosslinking of approximately 0.16 s^{-1}. As glucose levels increased, these networks exhibited significantly greater dynamics, as indicated by shifts in their ω_c and corresponding τ_r (Table S2†); however, this was not observed in the 4aPEG-GLD and 4aPEG-FLD networks. At 400 mg dL^{-1} glucose, the networks became more dynamic, with τ_r of the networks decreasing by an order of magnitude to values of approximately 0.6–1.0 s. In addition, there was no obvious impact on the resulting hydrogel properties due to the stereochemistry of the glycidol group used to prepare these *cis*-1,2 diols.

While PBA–diol networks prepared from the double *cis*-1,2 diol end groups were more glucose-responsive, they were also much less stiff than the networks prepared from GLD and FLD crosslinking. To better compare glucose-responsiveness for each hydrogel platform in a similar stiffness regime, networks of 4aPEG-GLD and 4aPEG-FLD hydrogels were also prepared at lower concentrations and studied by the same rheological testing (Fig. S15†). Specifically, 4aPEG-GLD was prepared at 3% (w/v) and 4aPEG-FLD was prepared at 5% (w/v) to achieve networks of comparable stiffness (7×10^2 Pa) to those prepared from the double *cis*-1,2 diol endgroups. In this reduced stiffness regime, the GLD crosslinking showed an 18% reduction in modulus at glucose conditions of 400 mg dL^{-1}, while the FLD crosslinking had a 59% reduction in modulus at this same glucose condition. Accordingly, some amount of glucose-responsive function was revealed in hydrogels with lower polymer content, and thus a lower density of network crosslinks. This is likely due to glucose being at a higher molar excess to PBA–diol crosslinks when polymer content was reduced, thus offering greater relative competition. These networks also demonstrated glucose-responsive network dynamics, evident from a rightward shift in ω_c with increasing glucose concentration that is characteristic of more dynamic networks. It is possible that network dynamics could be further tuned by mixing macromers bearing different diols, in line with other results shown when mixing macromers bearing different PBA motifs while keeping the diol conserved.[46]

3.4. Glucose-responsive insulin release

Glucose-responsive insulin release from the different PBA–diol hydrogels was next investigated. Hydrogels were prepared at 10% (w/v) as before, and a FITC-labelled insulin was encapsulated within the gel network to study its glucose-responsive release when gels were immersed in a bulk buffer of pH 7.4 that contained varying physiologically relevant glucose concentrations, ranging from 0 to 400 mg dL^{-1}, as previously done for other PBA–diol hydrogels.[31] Release was then quantified over time through monitoring fluorescence of the bulk phase (Fig. 4). The hydrogels prepared from the 4aPEG-GLD macromer exhibited very limited glucose-responsive insulin release (Fig. 4a), consistent with previous studies on this material when prepared at 10% (w/v).[11,31] The amount and rate of insulin release from the 4aPEG-GLD gel showed limited glucose-dependent behavior, with only a 10% increase in insulin release when comparing the two glucose concentration extrema (0 and 400 mg dL^{-1}) at the 8 h endpoint of the study. Similarly, the 4aPEG-FLD hydrogel displayed only a modest glucose-responsive insulin release behavior, with a 20% increase in release between the two glucose extrema at the 8 h endpoint of the study (Fig. 4b). Hydrogels prepared from the three double *cis*-1,2 diol structures demonstrated significantly enhanced insulin release in response to glucose, in each case accelerating release by approximately 50% between the two glucose extrema at the 8 h endpoint of the study (Fig. 4c–e). Of note, however, was that insulin leakage in these networks under conditions of no glucose was significantly higher than from either the GLD or FLD chemistries. Generally, insulin leakage in the glucose-free case corresponds to the observed moduli in rheology. As the extent of network crosslinking at equilibrium is correlated with the plateau modulus,[12] this finding indicates that insulin release from these networks is more restricted with a higher

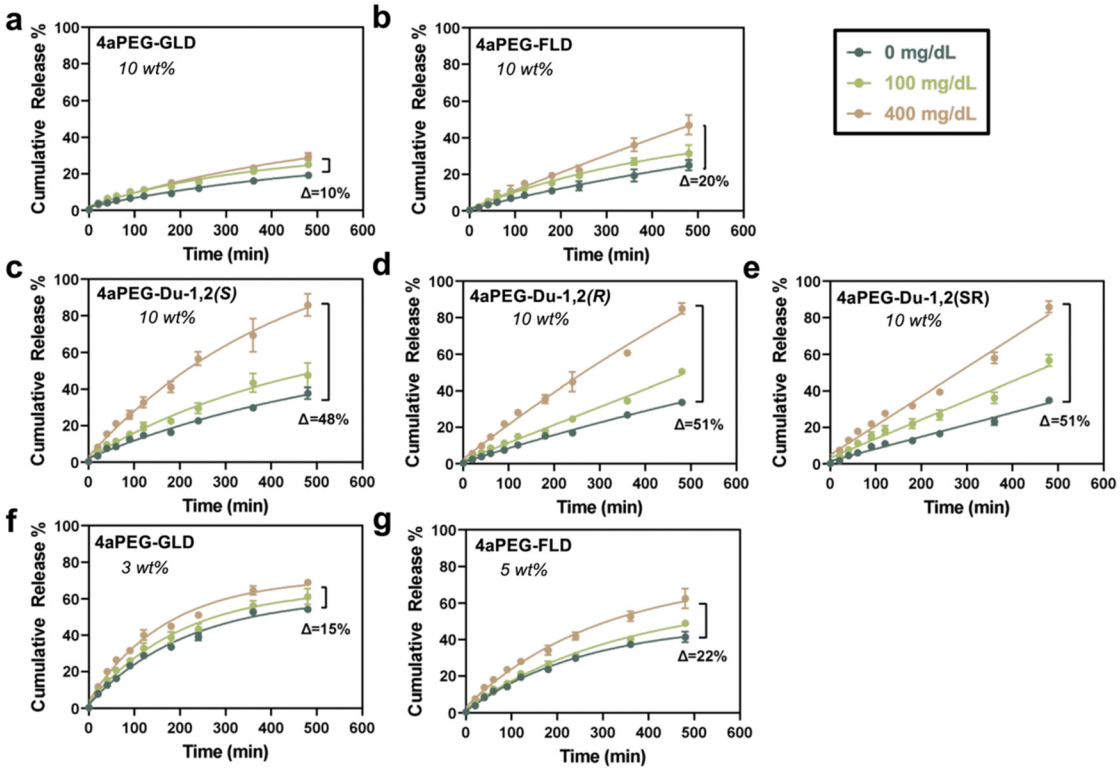

Fig. 4 Glucose-dependent FITC-insulin release from hydrogels prepared with 4aPEG-FPBA and different 4aPEG-diols. Samples were prepared at 10% (w/v) polymer from (a) 4aPEG-GLD, (b) 4aPEG-FLD, (c) 4aPEG-Du-1,2(*S*), (d) 4aPEG-Du-1,2(*R*), (e) 4aPEG-Du-1,2(*SR*). In addition, release from stiffness-matched control gels was studied from (f) 3% (w/v) 4aPEG-GLD and (g) 5% (w/v) 4aPEG-FLD. In all cases, each hydrogel was formulated in phosphate buffer (0.1 M, pH 7.4) and then placed into a bulk buffer containing 0–400 mg dL^{-1} glucose.

extent of network crosslinking. As insulin primarily exists as a ~35 kDa hexamer with a hydrodynamic diameter of 5.6 nm,[47] its passive release through the porosity of a 10 kDa PEG network prepared at 10% (w/v) with a pore dimension of 6.4 nm is more limited in the fully crosslinked case.[48] This phenomenon also explains why the networks with more glucose-responsive moduli likewise exhibit accelerated insulin release upon exposure to glucose, a desirable property of glucose-responsive materials. However, this also is a potential drawback in these designs, as insulin leakage in the absence of glucose, or at low glucose levels, is undesirable and could be dangerous in therapeutic applications.

To further validate the correlation between network modulus and glucose-responsive insulin release, the stiffness-matched GLD and FLD hydrogel formulations were also assessed for release of encapsulated FITC-insulin. Comparing the glucose-free case at different polymer concentrations, the 3% (w/v) GLD hydrogel showed increased insulin release of 55% (Fig. 4f) compared to 20% that had been released from the 10% (w/v) gels at 0 mg dL^{-1} (Fig. 4a). This finding again demonstrates that crosslink density dictates insulin release from these networks. The extent of glucose-responsive release in these networks remained limited, however; an increase of only 15% was observed upon increasing glucose concentration to 400 mg dL^{-1}, demonstrating that glucose still struggles to effectively compete with PBA–diol crosslinks prepared from GLD (Fig. 4f). The hydrogel prepared from 4aPEG-FLD also demonstrated an increase in release at 5% (w/v) compared to its previous study at 10% (w/v), and some slight increase in its glucose-responsive release at this lower concentration as well (Fig. 4g). However, PBA–diol crosslinks prepared from FLD also demonstrated limited glucose-responsive release even in the stiffness-matched case.

3.5. Small molecule binding affinity validation

Following the observation of varying glucose-responsive properties in these PBA–diol hydrogels, the binding affinities of the different diol derivatives to FPBA were quantified on the molecular scale using isothermal titration calorimetry (ITC). Model small molecule diol compounds ($[X]_{sm}$) were prepared using the same linkage approaches as were used to modify the PEG macromers. The binding affinity (K_{eq}) between FPBA and glucose was previously reported from ITC as 8.6 M^{-1}.[31] In contrast, the K_{eq} for FPBA binding to GLD_{sm} was 4922.0 M^{-1} (Fig. 5); at approximately 500 times higher than the interaction between FPBA and glucose, this result explains the limited glucose-responsive function of this bond upon competition from glucose under physiological conditions (*i.e.,* 5–20 mM glucose). The K_{eq} for FPBA binding to FLD_{sm} was reduced to 1176 M^{-1}; though somewhat lower than that for GLD_{sm}, this interaction is still well above that

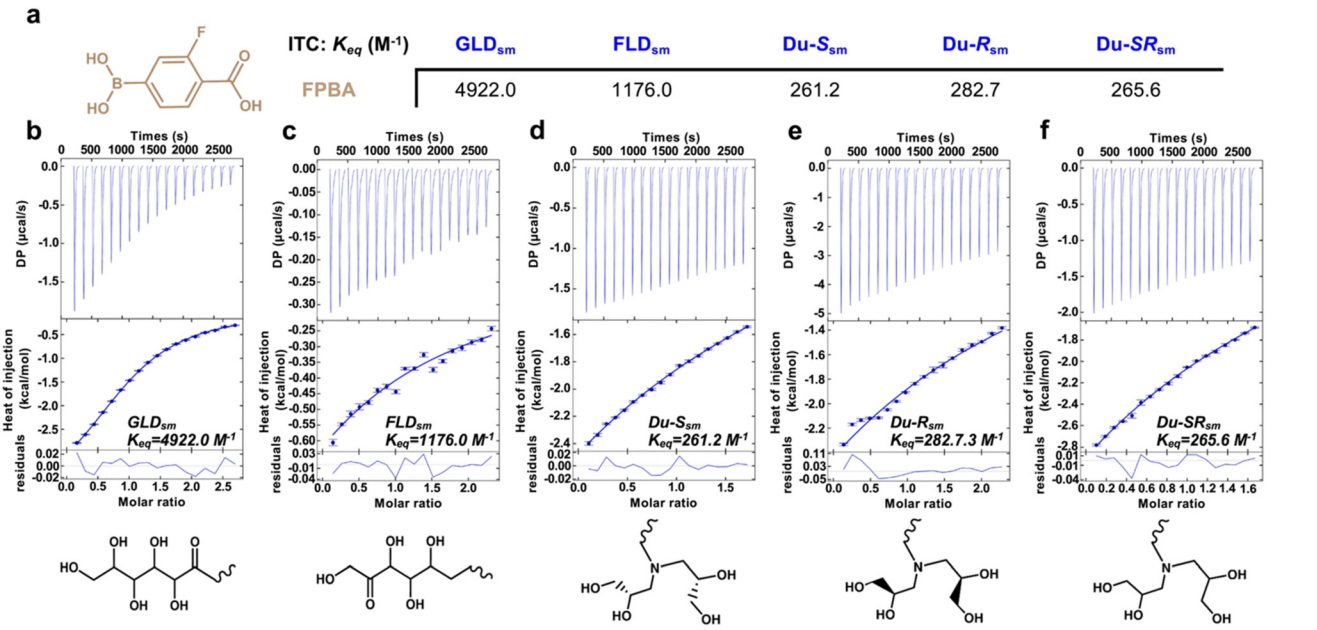

Fig. 5 Isothermal titration calorimetry (ITC) studies, showing (a) tabulated binding affinities (K_{eq}) quantified for binding between small molecule diol derivatives and FPBA, as well as representative model-fit data for binding of diol derivatives (b) GLD$_{sm}$, (c) FLD$_{sm}$, (d) Du-S_{sm}, (e) Du-R_{sm}, and (f) Du-SR_{sm}.

between FPBA and glucose, explaining the limited glucose-responsiveness of the FLD networks. Interestingly, this trend in binding affinity is reversed from the typical binding affinities for PBAs to normal glucose and fructose; FPBA was found to bind fructose with an affinity 80× that of glucose.[31] In comparison, the K_{eq} values between FPBA and Du-S_{sm}, Du-R_{sm}, and Du-SR_{sm} were 261.2 M^{-1}, 282.7 M^{-1}, and 265.6 M^{-1}, respectively. These values are more than an order of magnitude lower than those for GLD$_{sm}$. The lower binding affinities between these new diol derivatives and FPBA thus enable glucose to better compete and replace the diols under physiological concentrations, leading to enhanced glucose-responsiveness in the resulting materials. The reasons for the reduced affinity are unclear, as the valency of hydroxyl groups is similar across all diols examined by ITC. This suggests that differences in the spatial arrangement of these hydroxyl groups within the diol structures may influence their binding to PBA. Related work showed that the structure of alcohols, including the presence of neighboring groups like amides, can have implications on the affinity and dynamics of PBA–diol crosslinking.[49] The similar binding affinity for FPBA to Du-S_{sm}, Du-R_{sm}, and Du-SR_{sm} also indicates that the stereochemistry of attachment for these double-modified *cis*-1,2 diol derivatives had no significant effect on its interaction with FPBA, as also observed in rheology and release studies. These findings furthermore corroborate studies from rheology. Specifically the plateau modulus for these networks is related to the equilibrium bond formation, or K_{eq}, of the dynamic-covalent crosslinking interactions;[12] the trends previously observed for plateau modulus of the networks in the glucose-free case directly correspond to the measurements made from ITC. This study of affinity of the crosslinking motifs used to form each of these networks thus explains the molecular-scale origins of glucose-responsiveness arising from a reduction in the PBA–diol crosslinking of the network.

Conclusions

Here, diol chemistry was explored in PBA–diol crosslinked hydrogel networks for its impact of glucose-responsive properties. Rheological analysis and insulin release studies confirmed the importance of diol structure on the ability to both form stable hydrogels and afford competition from ambient glucose to disrupt the network structure and promote insulin release. These observations were corroborated by a study of the binding affinity of model small molecules to the PBA motif used for crosslinking. Overall, these findings highlight the efficacy of engineering diol derivatives with reduced binding affinity to PBA motifs, thereby improving the glucose-responsive properties of the resulting hydrogel materials through more effective glucose competition. Whereas a related approach sought to increase the binding affinity of glucose to the boronate crosslinking motif,[31] this work instead demonstrated a similar function by reducing the affinity of the PBA–diol crosslinks. The reduction in PBA–diol crosslinking affinity and its subsequent effects on the mechanical and dynamic properties of hydrogel networks did not appear to be related to the valency of hydroxyl groups, as demonstrated by comparing the GLD-derived diol to the double *cis*-1,2 diols formed from epoxide ring-opening reactions. However, a single *cis*-1,2 diol formed from one epoxide ring-opening reaction did not result in hydrogel formation, nor did a

single *cis*-1,3 diol. The stereochemistry of the epoxides used to form *cis*-1,2 diols also showed no effect. These findings thus suggest that the spatial arrangement of *cis*-1,2 diols likely underlies the observed differences in affinity and resulting network properties. This approach likewise illustrates limitations of commonly used PBA–diol crosslinking motifs, as these often have much higher affinity for synthetic diols used in preparing dynamic-covalent crosslinks than they do to glucose. By enhancing the sensitivity of PBA–diol interactions, the designed hydrogel materials have promise for applications in glucose-responsive insulin delivery systems.

Data availability

The data supporting this article have been included in the main text and online ESI.†

Conflicts of interest

The authors declare no conflicts of interest.

Acknowledgements

MJW gratefully acknowledges funding support for this work from Breakthrough T1D (5-CDA-2020-947-A-N), the Helmsley Charitable Trust (grants 2019PG-T1D016 and 2102-04994), the American Diabetes Association Pathway Accelerator Award (1-19-ACE-31), and a National Science Foundation CAREER award (BMAT, 1944875). We also acknowledge the NDEnergy Materials Characterization Facility for use of the rheometer and the Notre Dame Biophysics Facility for use of the ITC. Portions of Fig. 1 and the TOC graphic were prepared using BioRender.

References

1 J. Li and D. J. Mooney, *Nat. Rev. Mater.*, 2016, **1**, 16071.
2 N. A. Peppas, J. Z. Hilt, A. Khademhosseini and R. Langer, *Adv. Mater.*, 2006, **18**, 1345–1360.
3 A. S. Hoffman, *Adv. Drug Delivery Rev.*, 2012, **64**, 18–23.
4 M. J. Webber and M. W. Tibbitt, *Nat. Rev. Mater.*, 2022, **7**, 541–556.
5 S. Correa, A. K. Grosskopf, H. Lopez Hernandez, D. Chan, A. C. Yu, L. M. Stapleton and E. A. Appel, *Chem. Rev.*, 2021, **121**, 11385–11457.
6 S. M. Mantooth, B. G. Munoz-Robles and M. J. Webber, *Macromol. Biosci.*, 2019, **19**, e1800281.
7 E. A. Appel, M. W. Tibbitt, M. J. Webber, B. A. Mattix, O. Veiseh and R. Langer, *Nat. Commun.*, 2015, **6**, 6295.
8 J. K. Sahoo, M. A. VandenBerg and M. J. Webber, *Adv. Drug Delivery Rev.*, 2018, **127**, 185–207.
9 S. J. Rowan, S. J. Cantrill, G. R. L. Cousins, J. K. M. Sanders and J. F. Stoddart, *Angew. Chem., Int. Ed.*, 2002, **41**, 898–952.
10 S. Tang, B. M. Richardson and K. S. Anseth, *Prog. Mater. Sci.*, 2021, **120**, 100738.
11 V. Yesilyurt, M. J. Webber, E. A. Appel, C. Godwin, R. Langer and D. G. Anderson, *Adv. Mater.*, 2016, **28**, 86–91.
12 B. Marco-Dufort, R. Iten and M. W. Tibbitt, *J. Am. Chem. Soc.*, 2020, **142**, 15371–15385.
13 B. Marco-Dufort and M. W. Tibbitt, *Mater. Today Chem.*, 2019, **12**, 16–33.
14 S. Xian, M. A. VandenBerg, Y. Xiang, S. Yu and M. J. Webber, *ACS Biomater. Sci. Eng.*, 2022, **8**, 4873–4885.
15 R. C. Ollier, Y. Xiang, A. M. Yacovelli and M. J. Webber, *Chem. Sci.*, 2023, **14**, 4796–4805.
16 W. L. A. Brooks and B. S. Sumerlin, *Chem. Rev.*, 2016, **116**, 1375–1397.
17 Y. Dong, W. Wang, O. Veiseh, E. A. Appel, K. Xue, M. J. Webber, B. C. Tang, X.-W. Yang, G. C. Weir, R. Langer and D. G. Anderson, *Langmuir*, 2016, **32**, 8743–8747.
18 G. Springsteen and B. Wang, *Tetrahedron*, 2002, **58**, 5291–5300.
19 A. Matsumoto, S. Ikeda, A. Harada and K. Kataoka, *Biomacromolecules*, 2003, **4**, 1410–1416.
20 D. Shiino, Y. Murata, A. Kubo, Y. J. Kim, K. Kataoka, Y. Koyama, A. Kikuchi, M. Yokoyama, Y. Sakurai and T. Okano, *J. Controlled Release*, 1995, **37**, 269–276.
21 Y. Koyama, T. Okano and Y. Sakurai, *J. Controlled Release*, 1992, **19**, 161–170.
22 Y. Xiang, B. Su, D. Liu and M. J. Webber, *Adv. Ther.*, 2023, **7**, 2300127.
23 M. A. VandenBerg and M. J. Webber, *Adv. Healthcare Mater.*, 2019, **8**, e1801466.
24 Z. Ye, Y. Xiang, T. Monroe, S. Yu, P. Dong, S. Xian and M. J. Webber, *Biomacromolecules*, 2022, **23**, 4401–4411.
25 T. D. James, M. D. Phillips and S. Shinkai, *Boronic Acids in Saccharide Recognition*, Royal Society of Chemistry, 2006.
26 W. L. A. Brooks, C. C. Deng and B. S. Sumerlin, *ACS Omega*, 2018, **3**, 17863–17870.
27 C. Zhang, M. D. Losego and P. V. Braun, *Chem. Mater.*, 2013, **25**, 3239–3250.
28 S. Yu, Z. Ye, R. Roy, R. R. Sonani, I. Pramudya, S. Xian, Y. Xiang, G. Liu, B. Flores, E. Nativ-Roth, R. Bitton, E. Egelman and M. J. Webber, *Adv. Mater.*, 2024, **36**, 2470119.
29 D. H.-C. Chou, M. J. Webber, B. C. Tang, A. B. Lin, L. S. Thapa, D. Deng, J. V. Truong, A. B. Cortinas, R. Langer and D. G. Anderson, *Proc. Natl. Acad. Sci. U. S. A.*, 2015, **112**, 2401–2406.
30 A. Matsumoto, T. Ishii, J. Nishida, H. Matsumoto, K. Kataoka and Y. Miyahara, *Angew. Chem., Int. Ed.*, 2012, **9**, 2166–2170.
31 Y. Xiang, S. Xian, R. C. Ollier, S. Yu, B. Su, I. Pramudya and M. J. Webber, *J. Controlled Release*, 2022, **348**, 601–611.
32 S. Xian, Y. Xiang, D. Liu, B. Fan, K. Mitrová, R. C. Ollier, B. Su, M. A. Alloosh, J. Jiráček, M. Sturek, M. Alloosh and M. J. Webber, *Adv. Mater.*, 2024, **36**, e2308965.
33 C. A. Brautigam, H. Zhao, C. Vargas, S. Keller and P. Schuck, *Nat. Protoc.*, 2016, **11**, 882–894.
34 W. B. Turnbull and A. H. Daranas, *J. Am. Chem. Soc.*, 2003, **125**, 14859–14866.
35 A. Brown, *Int. J. Mol. Sci.*, 2009, **10**, 3457–3477.
36 D. Stauffer, A. Coniglio and M. Adam, in *Polymer Networks*, Springer Berlin Heidelberg, Berlin, Heidelberg, 2007, pp. 103–158.

37 Y. Nakagawa and I. Yukishige, *Adv. Carbohydr. Chem. Biochem.*, 2012, **68**, 1–58.
38 F. A. Saddique, A. F. Zahoor, S. Faiz, S. A. R. Naqvi, M. Usman and M. Ahmad, *Synth. Commun.*, 2016, **46**, 831–868.
39 S. M. M. Dadfar, S. Sekula-Neuner, V. Trouillet and M. Hirtz, *Adv. Mater. Interfaces*, 2021, **8**, 2002117.
40 P. Rani and R. Srivastava, *RSC Adv.*, 2015, **5**, 28270–28280.
41 R. I. Kureshy, S. Singh, N.-U. H. Khan, S. H. R. Abdi, E. Suresh and R. V. Jasra, *J. Mol. Catal. A: Chem.*, 2007, **264**, 162–169.
42 D. G. D. Galpaya, J. F. S. Fernando, L. Rintoul, N. Motta, E. R. Waclawik, C. Yan and G. A. George, *Polymer*, 2015, **71**, 122–134.
43 Shivani, B. Pujala and A. K. Chakraborti, *J. Org. Chem.*, 2007, **72**, 3713–3722.
44 W. C. Yount, D. M. Loveless and S. L. Craig, *J. Am. Chem. Soc.*, 2005, **127**, 14488–14496.
45 L. Zou, A. S. Braegelman and M. J. Webber, *ACS Appl. Mater. Interfaces*, 2019, **11**, 5695–5700.
46 V. Yesilyurt, A. M. Ayoob, E. A. Appel, J. T. Borenstein, R. Langer and D. G. Anderson, *Adv. Mater.*, 2017, **29**, 1605947.
47 S. Hvidt, *Biophys. Chem.*, 1991, **39**, 205–213.
48 S. T. Lust, D. Hoogland, M. D. A. Norman, C. Kerins, J. Omar, G. M. Jowett, T. T. L. Yu, Z. Yan, J. Z. Xu, D. Marciano, R. M. P. da Silva, C. A. Dreiss, P. Lamata, R. J. Shipley and E. Gentleman, *ACS Biomater. Sci. Eng.*, 2021, **7**, 4293–4304.
49 B. Kang and J. A. Kalow, *ACS Macro Lett.*, 2022, **11**, 394–401.